

## The structure of chalcogen pairs in silicon

This article has been downloaded from IOPscience. Please scroll down to see the full text article.

1989 J. Phys.: Condens. Matter 1 35

(<http://iopscience.iop.org/0953-8984/1/1/004>)

View [the table of contents for this issue](#), or go to the [journal homepage](#) for more

Download details:

IP Address: 171.66.16.89

The article was downloaded on 10/05/2010 at 15:44

Please note that [terms and conditions apply](#).

## The structure of chalcogen pairs in silicon

S Greulich-Weber, J R Niklas and J-M Spaeth

Fachbereich Physik, Universität-GH Paderborn, Warburger Strasse 100A,  
D-4790 Paderborn, Federal Republic of Germany

Received 27 June 1988

**Abstract.** The chalcogen pair centres  $(S-S)^+$  and  $(Se-Se)^+$  in Si were investigated with electron–nuclear double resonance (ENDOR). It was possible to resolve the superhyperfine interactions with 16 shells  $((S-S)^-)$  and 20 shells  $((Se-Se)^-)$  of  $^{29}Si$  neighbours as well as with the central Se nuclei. From the analysis, it follows that in both cases the chalcogen atoms occupy substitutional lattice sites and are very slightly pulled to each other by bonding. The spin distributions of the monomer and dimer chalcogen centres are very similar and show largely a vacancy character.

### 1. Introduction

Chalcogen impurities in Si form deep-level donors with energy levels near the middle of the band gap. They are of technological interest for infrared detection and for photovoltaic processes. Chalcogens have been investigated with optical spectroscopy (Wagner *et al* 1984) and by electron spin resonance (ESR) (Ludwig 1965, Grimmeiss *et al* 1983) and electron–nuclear double resonance (ENDOR) in their singly ionised form ( $S^+$ ,  $Se^+$  and  $Te^+$ ) (Ludwig 1965, Greulich-Weber *et al* 1984a, Niklas and Spaeth 1983). From the latter investigation a detailed knowledge of the electronic structure of the ground state could be obtained from the resolved superhyperfine (SHF) interactions with many shells of Si neighbours. From the ENDOR experiments, it could not be decided whether the chalcogen ions reside on substitutional lattice sites or on the tetrahedral interstitial site. Self-consistent total energy calculations by Beeler *et al* (1985) showed, however, that the substitutional sites are energetically clearly favoured.

The existence of chalcogen pair defects was also seen in the optical spectra (Wagner *et al* 1984). However, from ESR alone (Wörner and Schirmer 1984), it could not be decided what sites are occupied by the pair of chalcogen ions. It is the purpose of this investigation of the chalcogen pairs  $(S-S)^+$  and  $(Se-Se)^+$  to resolve with ENDOR the SHF interactions with the Si neighbours in order to determine the structure model of the pairs and to compare their electronic structure with those of the monomer defects. By means of photo-ESR and photo-ENDOR it was established that the pairs studied have the same energy levels as those known from optical experiments.

Pair defects are of fundamental interest as the smallest clusters possible. So far, there is very little known about the detailed structure of any pairs in Si let alone about the electronic structure. It seemed therefore worthwhile to start such investigations with these comparatively simple chalcogen pairs.

## 2. Experimental details

The crystals used in this study were partly prepared by Dr Zulehner (Wacker Chemitronic) by a vapour transport technique (Wagner *et al* 1984, Dietl *et al* 1981) and ourselves. S and Se were diffused into B-doped Si (floating-zone material; resistivity  $2 \Omega \text{ cm}$ ) at  $1200^\circ\text{C}$ . The diffusion was carried out for between 24 and 72 h. More pair centres than monomer centres were obtained by slow cooling ( $100^\circ\text{C h}^{-1}$ ). Te could only be incorporated by the vapour transport technique. ENDOR experiments were carried out at  $T = 17 \text{ K}$  in the approximate frequency ranges 3–20 MHz for the (S–S)<sup>+</sup> pair defect and 2–300 MHz for the (Se–Se)<sup>+</sup> pair defect with a custom-built computer-controlled X-band spectrometer. For details of the ENDOR measurement techniques and the digital handling of the experimental data see Greulich-Weber *et al* (1984b).

## 3. Experimental results

The ESR spectra of S<sup>+</sup>, (S–S)<sup>+</sup>, Se<sup>+</sup> and (Se–Se)<sup>+</sup> defects could be measured. The spectra agreed with those previously published (Ludwig 1965, Wörner and Schirmer 1984). The ESR spectra of the S<sup>+</sup> and (S–S)<sup>+</sup> defects as well as those for the corresponding Se defects overlapped considerably. In order to establish that the new lines appearing in addition to the known S<sup>+</sup> and Se<sup>+</sup> lines, respectively, are indeed due to pair centres, both photo-ESR and photo-ENDOR as well as ENDOR experiments were carried out. From optical data, it was found that the S<sup>+</sup> level is at  $E_v + 0.58 \text{ eV}$ , while the level  $E_v + 0.8 \text{ eV}$  was assigned to (S–S)<sup>+</sup> defects (Wagner *et al* 1984). In a sample with a higher B concentration the Fermi level was below both levels so that they were not occupied. ESR measurements are then only possible after electrons are raised from the valence bands into these levels by additional illumination. Figure 1 shows the photo-ESR signal as a function of the photon energy for the S<sup>+</sup> centre and the ESR line assigned to (S–S)<sup>+</sup>. The onset of ESR at 0.58 and 0.8 eV agrees very well with the energy levels assigned to these defects. Analogous experiments for Se<sup>+</sup> and (Se–Se)<sup>+</sup> pairs showed the same correlation. Thus, by photo-ESR a correlation between the optically determined energy levels and the ESR spectra could be achieved. Figure 2 shows the photo-ENDOR effect for S<sup>+</sup> and (S–S)<sup>+</sup> defects. ENDOR lines of both centres appear simultaneously because of the ESR line overlap, if both levels are occupied. However, for illumination with light below 0.8 eV only S<sup>+</sup> ENDOR lines appear. In this way also the ENDOR lines of the two different defects could be discriminated.

For a pair centre with an axis exactly along [111], there are three types of neighbour shell symmetry.

(i) The neighbour shell contains only one Si atom, which is on the [111] defect axis. This axis is the tensor  $z$  axis. The tensor is axial.

(ii) The neighbour shell contains three Si atoms, which are located around the defect axis. They are related to each other by a  $120^\circ$  rotation around this axis. There is one free angle  $\theta$  describing the tensor  $z$  axis orientation in a (110) plane. The tensor is axial. If the static magnetic field  $B_0$  is in the (110) plane, the SHF interactions for two of the three Si neighbours are identical.

(iii) The neighbour shell contains three Si atoms of low symmetry. There are three free angles  $\theta$ ,  $\varphi$ ,  $\gamma$ , describing the tensor orientation in a (110) plane. The tensor is non-axial.

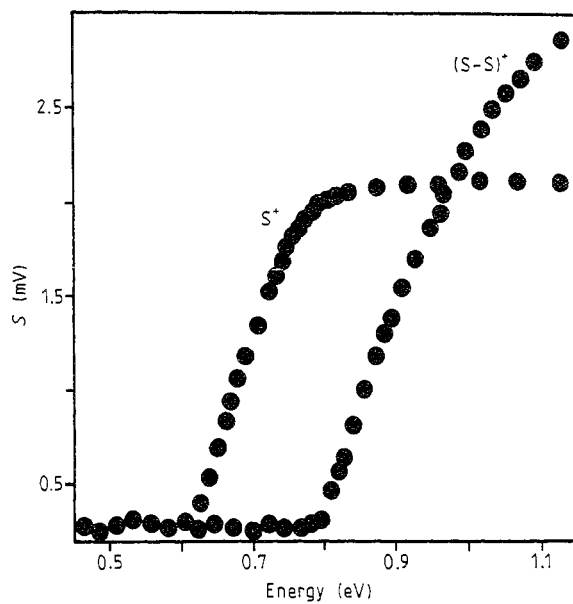


Figure 1. Photo-ESR signal as a function of photon energy for  $S^+$  and  $(S-S)^+$  centres in Si.

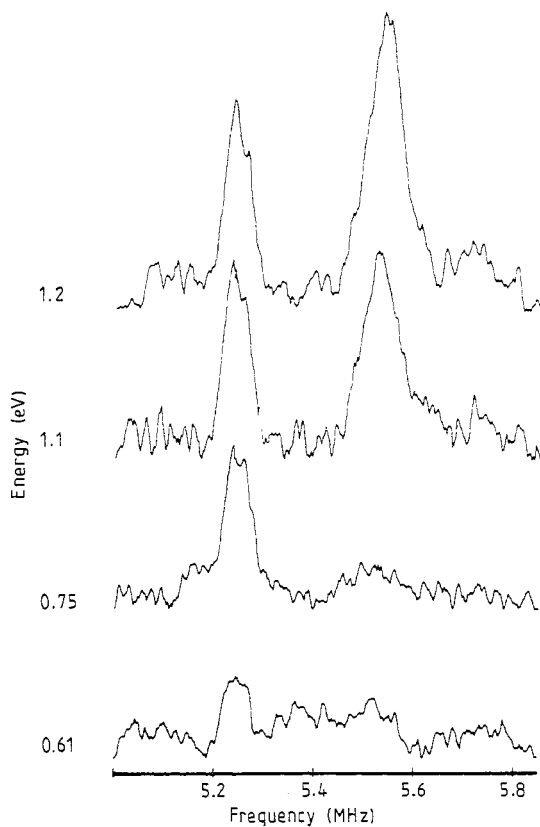
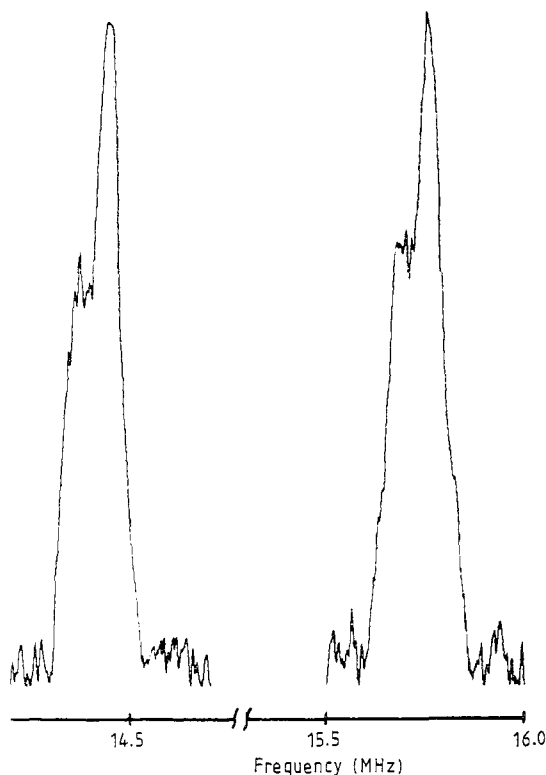


Figure 2. Part of a photo-ENDOR spectrum showing  $^{29}\text{Si}$  ligand interactions for  $S^+$  (at 5.25 MHz) and  $(S-S)^+$  (at 5.5 MHz) defects in Si.



**Figure 3.** The largest  $^{29}\text{Si}$  ligand interaction for the  $(\text{S-S})^+$  pair in Si showing a splitting with intensity ratios of 2:1 which indicates that at least three Si ligands cause this interaction.  $B_0 \parallel [100] + 4^\circ$  towards  $[111]$ .

A neighbour shell for a pair defect with central inversion symmetry contains twice the number of Si atoms of each symmetry type.

Owing to the four possible  $[111]$  orientations of the defect axis in the Si crystal the angular dependence plot for the type (i) symmetry looks like a regular  $[111]$  neighbour shell symmetry. The pattern is very complicated for symmetry type (ii), if the tensor  $z$  axes are not precisely parallel to  $[111]$  directions. Figure 3 shows a part of the ENDOR spectrum of the largest SHF interaction, belonging to the nearest  $[111]$  neighbours for the  $(\text{S-S})^+$  pair centre. The magnetic field orientation is  $[100] + 4^\circ$  towards  $[111]$  in a  $(110)$  plane. The small splitting of the lines at 14.4 and 15.7 MHz into two components with an intensity ratio of 2:1 clearly indicates that these lines correspond to type (ii) symmetry. There must be at least three Si nuclei causing this splitting. In fact there are six nuclei giving rise to the lines due to the central inversion symmetry. This splitting proves that we have indeed a pair centre and not a monomer centre, where four nuclei would be seen instead of three.

As can be seen from table 1, no type (i) symmetry ligands were found at least down to SHF interactions of about 0.3 MHz.

For the  $(\text{Se-Se})^+$  centres a hyperfine (HF) interaction with the  $^{34}\text{Se}$  nuclei (5.58% abundance;  $I = \frac{1}{2}$ ) is resolved by ESR and could also be measured precisely with ENDOR in the frequency range between 280 and 300 MHz.

The Se-HF interaction measured with ENDOR shows that the paramagnetic Se centre

**Table 1.** HF and SHF interaction data for chalcogen pairs in Si. The tensor angle  $\theta$  is given with respect to [110] directions or  $z \parallel [111]$ ; the angles  $\theta$  are  $54.74^\circ$  and  $35.26^\circ$ , respectively. The symmetry of the shells where  $\theta$  is in parentheses could not be precisely determined.

Si: (Se-Se) <sup>-</sup>							Si: (S-S) <sup>+</sup>						
Type	<i>a</i> (MHz)	<i>b</i> (MHz)	<i>b'</i> (MHz)	$\theta$ (deg)	$\gamma$ (deg)	$\varphi$ (deg)	Type	<i>a</i> (MHz)	<i>b</i> (MHz)	<i>b'</i> (MHz)	$\theta$ (deg)	$\gamma$ (deg)	$\varphi$ (deg)
i	606.700	5.655					i	—	—				
ii	21.690	5.440	0	35.4			ii	23.854	4.875	0	34.9		
ii	12.675	0.471	-0.096	57.8			ii	11.834	0.428	-0.090	56.2		
iii	8.176	0.448	-0.105	21.6	-4.3	49.6	ii	8.441	0.460	-0.004	23.0		
ii	8.228	0.442	-0.062	21.6			iii	8.584	0.442	-0.175	22.7	-5.3	49.8
iii	-3.106	0.264	0.178	55.3	20.6	-5.2	iii	-2.057	0.196	-0.026	58.8	9.9	-11.4
iii	5.311	0.195	0.018	27.2	20.7	-0.7	iii	5.345	0.164	<0.002	26.8	2.1	0.2
iii	1.469	0.078	0.005	50.2	19.2	-0.9	iii	1.505	0.143	0.133	59.5	20.4	0.6
iii	0.593	0.078	-0.035	48.2	65.8	-10.9	iii	0.432	0.051	<0.002	63.0	12.0	4.0
iii	5.796	0.074	0.044	63.6	19.8	13.8	ii	5.336	0.048	<0.002	28.0		
ii	5.235	0.059	0.009	67.3			iii	0.668	0.032	-0.010	71.0	15.0	8.0
ii	-0.600	0.038	<0.002	21.8			iii	4.728	0.030	0.007	67.0	25.0	11.0
	2.294	0.018	0.010	(61)				0.929	0.017	<0.002	(61)		
	1.956	0.018	-0.005	(23)				0.300	0.003	<0.002	(61)		
	0.897	0.017	-0.006	24.0				1.083	0.002	<0.002	(61)		
	1.179	0.015	-0.009	(21)				0.800	0.002	<0.002	(56)		
	1.049	0.003	<0.002	(61)									
	0.429	<0.002	<0.002	(61)									
	0.358	<0.002	<0.002	(61)									
	0.303	<0.002	<0.002	(61)									

is exactly oriented along a [111] axis. The HF data are in good agreement with those measured by Wörner and Schirmer (1984) by ESR. Both defect atoms have identical HF interactions.

In order to determine the SHF interactions with the <sup>29</sup>Si ligands the angular dependences of the ENDOR lines were measured and analysed with the following spin Hamiltonian:

$$H = \mu_B g_e B_0 \cdot S + \sum_k \{ S \cdot A_k I_k - g_{nk} \mu_n B_0 \cdot I_k \} \quad (1)$$

where the symbols have their usual meanings. The results for both centres investigated are given in table 1 in terms of the isotropic SHF constants *a* and the anisotropic constants *b* and *b'*. They are related to the principal values of the SHF tensor **A** by

$$A_{xx} = a - b + b' \quad A_{yy} = a - b - b' \quad A_{zz} = a + 2b. \quad (2)$$

The constant *b'* describes the deviation from axial symmetry of the tensor **A**. The Euler angles  $\theta$ ,  $\gamma$  and  $\varphi$  in table 1 describe the orientations of the principal-axis systems of the tensors with respect to [110], [011] and [101].

Figure 4 shows an example of the excellent agreement between the angular dependences calculated with the data in table 1 (full lines) and the experimental ENDOR line positions (full squares) for the (S-S)<sup>+</sup> defects.

The symmetry of the neighbouring shells where  $\theta$  is given in parentheses in table 1 could not be clearly identified owing to their very small anisotropic interactions. The

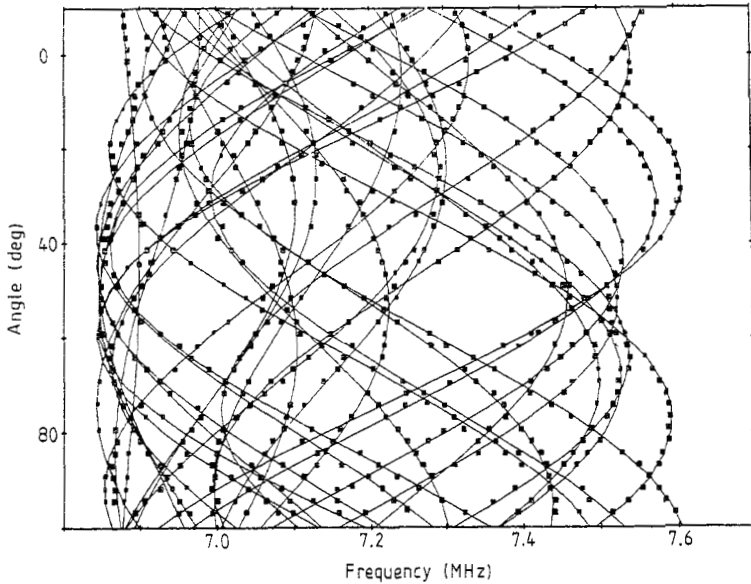


Figure 4. Example for the calculated angular dependences (—) and the experimental ENDOR line positions (■) for the  $(S-S)^{-}$  pair defect.

relative signs of  $a$  and  $b$  turned out to be different for some shells. From the experiments the absolute signs cannot be determined.

The ENDOR analysis clearly shows that there are  $(S-S)^{+}$  and  $(Se-Se)^{+}$  pair centres where each  $S^{+}$  and  $Se^{+}$ , respectively, is surrounded by three  $(110)$ -symmetry Si neighbours, which are in  $(110)$  mirror planes of the defect. Whether the two chalcogens 'share' a substitutional site (interstitial model) or are both on substitutional sites cannot be decided from the experiment alone. Because of the ligand symmetries found, it is not possible that one chalcogen is substitutional and the other one interstitial. The following discussion of the data will show that in both cases the chalcogen atoms reside on substitutional sites.

We have not been able to observe  $(Te-Te)^{+}$  pairs despite many efforts to produce them. The failure to observe them is in agreement with recent theoretical calculations by Weinert and Scheffler (1987) in which it is predicted that  $(Te-Te)^{+}$  pairs are not stable while the calculation predicts stability for  $(S-S)^{+}$  and  $(Se-Se)^{+}$  centres.

## 4. Discussion

### 4.1. Structure model of the pair centres

The SHF interactions of both  $(S-S)^{+}$  and  $(Se-Se)^{+}$  centres are very similar (table 1), which suggests that both pair centres occupy the same sites. The fact that they are indeed pairs follows from the exact  $[111]$  symmetry of the Se HF interaction and from the fact that there are three Si ligands with the largest SHF interactions in  $(110)$  symmetry (type (ii)) and not four as a monomer centre would have.

An ESR identification of the  $(Se-Se)^{+}$  pair defect by Wörner and Schirmer was based on the intensities of the HF lines of both Se nuclei which both have the same HF interaction.

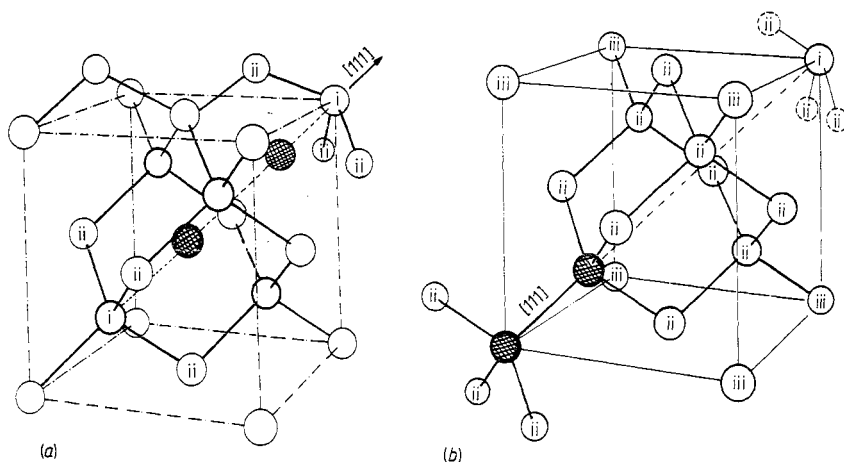


**Figure 5.** Model for (a) an interstitial–interstitial pair defect and (b) a substitutional–substitutional pair defect. The symbols in the circles denote the  $^{29}\text{Si}$  symmetry type explained in the text.

Even with the high resolution of the ENDOR method, we observed no difference between the HF interactions of both Se nuclei. Since only one HF interaction was found, both Se nuclei must occupy equivalent sites or, in other words, the wavefunction of the unpaired electron must have a mirror plane perpendicular to the connection line between the two Se (S) nuclei. Therefore a combination of a lattice site and an interstitial site is not possible. There are only two possible sites for the chalcogen nuclei of the pair centre: either both occupy interstitial sites as shown in figure 5(a) or both occupy substitutional sites as in figure 5(b).

In the interstitial model there would be two Si neighbours along the  $\langle 111 \rangle$  chalcogen connection line as nearest neighbours and one would have expected to see type (i) Si nuclei with a pronounced interaction. No such interaction was found (table 1). In fact, if such an interaction existed, then it would occur only for SHF constants of  $a < 1$  MHz and  $b < 0.03$  MHz, which would be too low to have been detected. According to figure 5(a) the type (i) nuclei are nearest neighbours to one chalcogen and to the three nearest Si of type (ii). It would be very strange that such a neighbour should have such a small undetectable interaction, while 20 shells were measured farther away from the chalcogen with larger interactions. From a comparison with  $\text{S}^+$  and  $\text{Se}^+$  monomer centres (Greulich-Weber *et al* 1984a), one would also expect larger interactions for a nearest-neighbour Si. The minimum interaction which one would have to see for the two type (i) nuclei would be the classical point dipole–dipole interaction caused there by the unpaired electron distribution. The largest contribution would come from the three Si with about 35% localisation as calculated from the measured SHF interactions (see below), which are nearest neighbours to the type (i) nuclei and from about 3% localisation at the chalcogen. This gives a value of approximately 0.25 MHz for  $b$  at site (i), which would easily have been detected, even if its isotropic SHF constant  $a$  is zero. We therefore exclude the interstitial model in agreement with theory, which predicts the lattice site model as the most stable (Weinert and Scheffler 1987). For the substitutional model (figure 5(b)) the type (i) nuclei are very far away. Their classical point dipole–dipole interaction is estimated to be  $b = 0.02$  MHz. For a small  $a$  (which is expected there), such a shell could not be safely identified. Between the nearest-neighbour Si shells and



the symmetry type (i) neighbour, we expect 12 shells of symmetry types (ii) and (iii) from the lattice model in figure 5(b). Nine neighbour shells of symmetry types (ii) and (iii) could be clearly identified.

For the nearest-Si-neighbour nuclei (type (ii)) the  $z$  axis deviates by  $0.37^\circ$  from the [111] orientation for (S-S)<sup>+</sup> and by  $0.2^\circ$  for (Se-Se)<sup>+</sup> centres. This deviation can have two causes.

(i) The two chalcogen atoms are slightly pulled towards or repelled from each other.

(ii) Since both chalcogen atoms of the pair have the same unpaired spin density and both contribute to the anisotropic SHF interaction, a deviation from the [111] orientation is expected.

However the influence of the second chalcogen atom on the neighbours of the first chalcogen atom will be very small owing to the  $1/r^3$  dependence of the dipole-dipole interaction and the small spin localisation at the chalcogen atom itself (see below). If the spin distribution on both chalcogen atoms causes the major effect for the  $z$  axis deviation, then the (S-S)<sup>+</sup> and (Se-Se)<sup>+</sup> pairs should show the same angle since both spin distributions are almost identical. We conclude, therefore, that the distortion is probably the larger influence; since the deviation of (S-S)<sup>+</sup> is nearly double that of (Se-Se)<sup>+</sup> and since the ionic radius of S<sup>+</sup> is smaller than that of Se<sup>+</sup>, it is expected that a small bonding distortion occurs in both cases and that it is smaller for the Se case. A repulsive distortion would be smaller for (S-S)<sup>+</sup> and it is physically not likely anyway in view of the pair formation. An upper limit of this effect of bonding distortion would be  $0.015 \text{ \AA}$  for (S-S)<sup>+</sup> and  $0.008 \text{ \AA}$  for (Se-Se)<sup>+</sup> as the deviation of each chalcogen atom from the lattice site towards each other.

We therefore conclude that from the ENDOR investigation we can say that the two chalcogen atoms reside on substitutional lattice sites, are slightly pulled together through bonding and have a symmetrical ground-state wavefunction with a mirror plane perpendicular to its connection line.

#### 4.2. Spin-density distribution

There is no complete theory yet available for the interpretation of the experimental SHF data of the chalcogen centres. A calculation of the isotropic SHF constant by Ren *et al* (1982) for S<sup>+</sup> centres showed that the wavefunction falls off monotonically over the first four shells followed by two oscillations up to the eleventh shell in rather good agreement with experimental data (Ludwig 1965, Niklas and Spaeth 1983, Greulich-Weber *et al* 1984a).

However, most of the unpaired spin density resides in Si  $p$  orbitals, giving rise to the anisotropic SHF constants. This was not calculated by Ren *et al*.

There is no theory on any SHF data for pair centres. In order to get a rough idea of how the spin-density distributions of monomer and dimer centres can be compared the simple approach of the linear combination of atomic orbitals was adopted to describe the experimental findings. From the experimental data the localisation of the unpaired electron in the  $i$ th neighbour shell is calculated according to

$$\bar{n}_i^2 = (|a_i|/|a_f| + |b_i|/|b_f|)N_i \quad (3)$$

with  $a_i$  and  $b_i$  the experimental values,  $a_f = 4150 \text{ MHz}$  and  $b_f = 101 \text{ MHz}$  the isotropic and anisotropic constants, respectively, of the free Si atom (Watkins 1975) and  $N_i$  the number of nuclei in each shell.

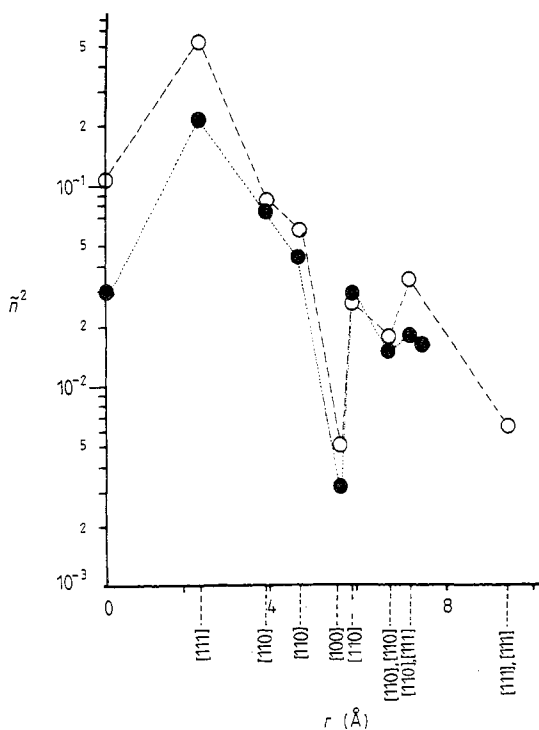


**Figure 6.** Spin-density distributions for  $\text{Se}^-$  (●, ·····) and  $(\text{Se-Se})^+$  (○, ----) pairs in Si. For details, see text.

The assumption of a monotonic decreasing spin density from the first shell (highest localisation) to the fourth shell enables an unambiguous assignment of the interactions to certain shells and distances. Figure 6 shows this for  $\text{Se}^+$  (open circles) according to ENDOR data from Greulich-Weber *et al* (1984a). Because of the lower symmetry of the pair centres, it is not obvious how a comparison should be made. We have chosen the following representation: since the spin distribution of the pair centre is symmetrical about a mirror plane between two chalcogen atoms, it can be represented as a superposition of two monomer defects centred one at each of the two chalcogen atoms. In this way the unpaired spin density in the neighbours is analogous to those of the monomer centres; the relative geometry is not influenced. The shells of the pair defect are a combination of those of a monomer defect from which they were formed by symmetry lowering. In comparison with the monomer, there is a different number of nuclei in a shell, however, e.g. the nearest-neighbour shell contains six instead of four nuclei as for the monomer. Therefore the number of pair centre nuclei in the shells and centre was normalised to that of the monomers. The spin-density distribution thus obtained (figure 6, full circles) shows a remarkable feature. From the second shell onwards, monomer and dimer centres differ very little in the spin-density distribution. The fact that for the pairs the nearest-neighbour density is about half that of the monomers is, of course, due to the distribution of the unpaired electron onto two chalcogen atoms instead of one. Thus the symmetry lowering of the pair in comparison with the monomer affects only a very small part of the lattice surroundings.

Since for both the monomer and the dimer centres, there is only a small localisation of spin density at the centre (10% and 6% on both central pair nuclei, respectively), it

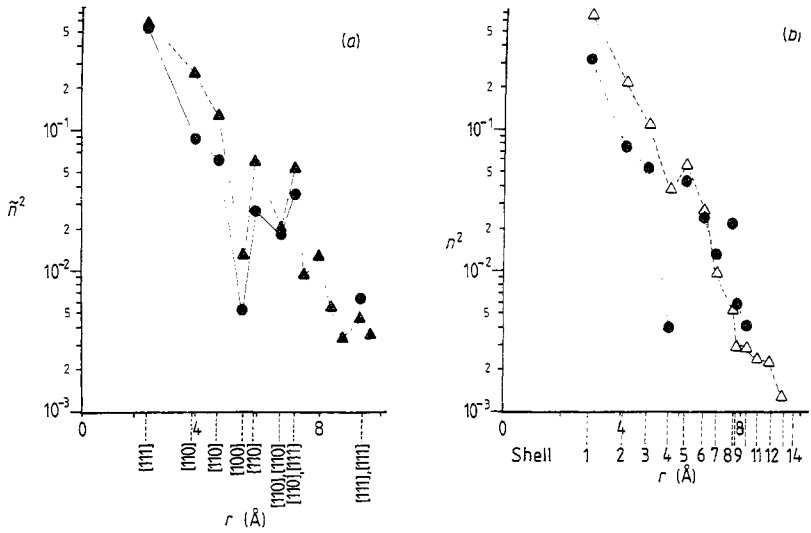


**Figure 7.** Spin-density distributions (a) for  $V^-$  ( $\blacktriangle$ , ----) and  $Se^+$  ( $\bullet$ , —) defects in Si and (b) for  $(V-V)^-$  ( $\triangle$ , ----) and  $(Se-Se)^+$  ( $\bullet$ , ..... ) defects in Si. For details, see text.

is tempting to compare their spin distributions with that of the vacancy and the divacancy, respectively. ENDOR data for both are available (Sprenger *et al* 1983, Sieverts *et al* 1978). A difficulty is, that  $V^-$  and  $(V-V)^-$  are both Jahn–Teller distorted and have lower symmetries, as have the two chalcogen defects. However, if for a qualitative comparison one neglects these distortions and adds the spin densities of those ligands to one shell, which would exist without the distortion in a shell, as was done to compare  $Se^+$  and  $(Se-Se)^+$ , figure 7 is obtained. It is indeed remarkable how similar the spin distributions of  $V^-$  and  $Se^+$  and those of  $(V-V)^-$  and  $(Se-Se)^+$  are. Since the spin distributions of the chalcogen centres themselves are almost indistinguishable, it can be said that both monomer and dimer chalcogen centres have a ground-state electronic structure which has a marked vacancy character. To our knowledge, this is the first time that this has been so clearly seen. There then remains the large question of why oxygen behaves so differently. So far, no substitutional  $O^+$  nor a pair-like  $(O-O)^+$  has been detected.

### Acknowledgments

The authors gratefully acknowledge support by the Deutsche Forschungsgemeinschaft and by Dr W Zulehner, Chemitronic, who provided many samples. We thank H Overhof for many helpful discussions.

### References

- Beeler F, Scheffler M, Jepsen O and Gunnarsson O 1985 *Proc. Conf. Mater. Res. Soc.* **46** 117
- Dietl J, Helmreich D and Sirtl E 1981 *Crystals Growth, Properties and Applications* vol 5 (Berlin: Springer)
- Greulich-Weber S, Niklas J R and Spaeth J-M 1984a *J. Phys. C: Solid State Phys.* **17** L991
- Greulich-Weber S, Niklas J R, Weber E R and Spaeth J-M 1984b *Phys. Rev. B* **30** 6292
- Grimmeiss H G, Janzen E, Ennen E, Schirmer O F, Schneider J, Wörner R, Holm C, Sirtl E and Wagner P 1983 *Phys. Rev. B* **24** 4571

Ludwig G W 1965 *Phys. Rev.* **137** A1520

Niklas J R and Spaeth J-M 1983 *Solid State Commun.* **46** 121

Ren Shang Yuan, Wei Min Hu, Sankey O F and Dow J D 1982 *Phys. Rev. B* **26** 951

Sieverts E G, Muller S H and Ammerlaan C A J 1978 *Phys. Rev. B* **18** 6834

Sprenger M, Muller S H and Ammerlaan C A J 1983 *Physica B* **116** 224

Wagner P, Holm C and Sirtl E 1984 *Festkörperprobleme (Advances in Solid State Physics)* vol 24, ed. P Grosse (Braunschweig: Vieweg) p 191

Watkins G 1975 *Point Defects in Solids* vol 2, ed. J H Crawford Jr and C M Slifkin (New York: Plenum)

Weinert C and Scheffler M 1987 *Phys. Rev. Lett.* **58** 1456

Wörner R and Schirmer O F 1984 *Solid State Commun.* **51** 9